Piezoelectric Structural Vibration Control

Marcelo A. Trindade

Abstract Over the last two decades, piezoelectric materials have been extensively used as components in active and passive structural vibration control solutions. The most frequent applications consider piezoceramic thin patches bonded to thin structures subjected to bending. For active vibration control solutions, the piezoceramic patches can be used as strain sensors and/or bending actuators when connected to properly designed signal conditioning, processing, and amplification. For passive vibration control solutions, they can be used as vibration dampers and/or absorbers when connected to properly designed electronic shunt circuits. The objective of this chapter is to present some examples of the use of piezoelectric materials, as distributed sensors and actuators, for the development and implementation of passive and active vibration control solutions.

Keywords Piezoelectric structures • Electromechanical coupling • Piezoelectric sensors and actuators • Piezoelectric shunted damping • Piezoelectric active control

1 Introduction

Over the last two decades, piezoelectric materials have been extensively used as components in active and passive structural vibration control solutions. The most frequent applications consider piezoceramic thin patches bonded to thin structures subjected to bending. For active vibration control solutions, the piezoceramic patches can be used as strain sensors and/or bending actuators when connected to properly designed signal conditioning, processing, and amplification. For passive vibration control solutions, they can be used as vibration dampers and/or absorbers when connected to properly designed electronic shunt circuits. The objective of this chapter is to present some examples of the use of piezoelectric materials,

M.A. Trindade (✉)
Department of Mechanical Engineering, São Carlos School of Engineering, University of São Paulo, Av. Trabalhador São-Carlense, 400, São Carlos, SP 13566-590, Brazil
e-mail: trindade@sc.usp.br

V. Lopes Junior et al. (eds.), *Dynamics of Smart Systems and Structures*,
DOI 10.1007/978-3-319-29982-2_12

as distributed sensors and actuators, for the development and implementation of passive and active vibration control solutions. Other textbooks discussing some of the topics presented in this chapter can be recommended (Meirovitch 1990; Preumont 1997, 2006; Reza Moheimani and Fleming 2006; Leo 2007).

2 Passive Vibration Control Using Piezoelectric Materials

For thin flexible structures, such as beams, plates, shells, and panels, most part of the vibrating energy is in bending motion and, thus, it seems worthwhile to make use of patches and/or layers of functional materials that can bend (deform) together with the structure and are capable of extracting (converting) this deformation energy from the host structure. To this end, piezoelectric materials are an interesting choice since they are quite effective in converting deformation energy into electrical energy. If connected to properly designed electric circuits, this electrical energy could then be extracted from the piezoelectric material. The seminal work of Hagood and von Flotow (1991) proposed the use of piezoelectric patches connected to resistive shunt circuits, leading to an equivalent vibration damper (in which the electrical energy is dissipated in the circuit resistance), or to resonant (resistive-inductive) shunt circuits, leading to an equivalent vibration absorber (in which the electrical energy is absorbed by the circuit within a narrow frequency range).

Later, studies focused mainly on the optimization of the shunt circuits by including resistances, inductances, capacitances, and switches in series and/or parallel (Lesieutre 1998; Clark 2000; Reza Moheimani 2003; Viana and Steffen 2006; Lallart et al. 2008). Other studies focused on the optimization of the electromechanical coupling between the piezoelectric materials and host structure (Trindade and Maio 2008; Trindade and Benjeddou 2009; Godoy and Trindade 2011).

2.1 Coupled Formulation for Structure, Piezoelectric Patches, and Shunt Circuits

In this section, a general methodology for the variational formulation of coupled equations of motion for structures with piezoelectric materials is presented. Equations are written in terms of both electric potential and electric charge in the piezoelectric elements. Equipotentiality over each piezoelectric element electrodes is accounted for in both formulations. Finally, a methodology for coupling the piezoelectric elements with electric circuits is presented.

2.1.1 Electric Potential Formulation

First, a formulation considering structure's generalized displacements and electric potential in the piezoelectric elements as variables is proposed. The virtual work done by internal forces can be found from the virtual variation of the electromechanical potential energy. In this first formulation, it is chosen to write the potential energy as the electric Gibbs energy, written in terms of mechanical strains $\boldsymbol{\varepsilon}$ and electric fields $\mathbf{E}$, such that its variation reads

$$\delta U(\boldsymbol{\varepsilon}, \mathbf{E}) = \int_{\Omega} \left(\delta\boldsymbol{\varepsilon}^{\mathrm{t}} \mathbf{c}^{E} \boldsymbol{\varepsilon} - \delta\boldsymbol{\varepsilon}^{\mathrm{t}} \mathbf{e} \mathbf{E} - \delta\mathbf{E}^{\mathrm{t}} \mathbf{e}^{\mathrm{t}} \boldsymbol{\varepsilon} - \delta\mathbf{E}^{\mathrm{t}} \boldsymbol{\varepsilon}^{\varepsilon} \mathbf{E} \right) \mathrm{d}\Omega, \tag{1}$$

where $\mathbf{c}^{E}$, $\mathbf{e}$, and $\boldsymbol{\varepsilon}^{\varepsilon}$ are the matrices of elastic (for constant electric field), piezoelectric, and dielectric (for constant mechanical strain) constants of the material.

Using appropriate kinematic assumptions for the piezoelectric structure to be studied and performing any form of spatial discretization, the coupled equations of motion can be derived in the form

$$\begin{bmatrix} \mathbf{M}_{\mathrm{s}} + \mathbf{M}_{\mathrm{p}} & 0 \\ 0 & 0 \end{bmatrix} \begin{Bmatrix} \ddot{\mathbf{u}} \\ \ddot{\mathbf{V}} \end{Bmatrix} + \begin{bmatrix} \mathbf{K}_{\mathrm{us}} + \mathbf{K}_{\mathrm{up}}^{E} & -\mathbf{K}_{\mathrm{uv}} \\ -\mathbf{K}_{\mathrm{uv}}^{\mathrm{t}} & -\mathbf{K}_{\mathrm{v}} \end{bmatrix} \begin{Bmatrix} \mathbf{u} \\ \mathbf{V} \end{Bmatrix} = \begin{Bmatrix} \mathbf{F}_{\mathrm{m}} \\ 0 \end{Bmatrix}, \tag{2}$$

where $\mathbf{M}_{\mathrm{s}}$ and $\mathbf{K}_{\mathrm{us}}$ are the mass and elastic stiffness matrices of the structure (without piezoelectric elements) and $\mathbf{M}_{\mathrm{p}}$ and $\mathbf{K}_{\mathrm{up}}^{E}$ are the mass and elastic (for constant electric fields) stiffness matrices of the piezoelectric elements. $\mathbf{K}_{\mathrm{uv}}$ and $\mathbf{K}_{\mathrm{v}}$ are the piezoelectric and dielectric stiffnesses of the piezoelectric elements. $\mathbf{F}_{\mathrm{m}}$ is a vector of the mechanical loads applied to the structure. The degrees of freedom (dofs) $\mathbf{u}$ are the generalized displacements and $\mathbf{V}$ are the generalized differences of electric potentials (voltages) on the piezoelectric material.

To account for the equipotential condition on the electrodes of each piezoelectric element, let us define the vectors of differences of electric potentials $\mathbf{V}_{\mathrm{p}}$ induced or applied to the electrodes of the piezoelectric elements, such that

$$\mathbf{V} = \mathbf{L}_{\mathrm{p}} \mathbf{V}_{\mathrm{p}}. \tag{3}$$

The boolean matrix $\mathbf{L}_{\mathrm{p}}$ has dimension $N \times N_{\mathrm{p}}$, where N is the number of spatial (nodal) points and N_{p} is the number of independent piezoelectric elements. $\mathbf{L}_{\mathrm{p}}$ allows to set an equal value to selected nodal differences of electric potentials.

Substituting Eq. (3) into Eq. (2) and pre-multiplying the second line of the resulting equation by $\mathbf{L}_{\mathrm{p}}^{\mathrm{t}}$ leads to

$$\begin{bmatrix} \mathbf{M}_{\mathrm{s}} + \mathbf{M}_{\mathrm{p}} & 0 \\ 0 & 0 \end{bmatrix} \begin{Bmatrix} \ddot{\mathbf{u}} \\ \ddot{\mathbf{V}}_{\mathrm{p}} \end{Bmatrix} + \begin{bmatrix} \mathbf{K}_{\mathrm{us}} + \mathbf{K}_{\mathrm{up}}^{E} & -\overline{\mathbf{K}}_{\mathrm{uv}} \\ -\overline{\mathbf{K}}^{\mathrm{t}}{}_{\mathrm{uv}} & -\overline{\mathbf{K}}_{\mathrm{v}} \end{bmatrix} \begin{Bmatrix} \mathbf{u} \\ \mathbf{V}_{\mathrm{p}} \end{Bmatrix} = \begin{Bmatrix} \mathbf{F}_{\mathrm{m}} \\ 0 \end{Bmatrix}, \tag{4}$$

where

$$\overline{\mathbf{K}}_{\mathrm{uv}} = \mathbf{K}_{\mathrm{uv}}\mathbf{L}_{\mathrm{p}}, \quad \overline{\mathbf{K}}_{\mathrm{v}} = \mathbf{L}_{\mathrm{p}}^{\mathrm{t}}\mathbf{K}_{\mathrm{v}}\mathbf{L}_{\mathrm{p}}. \tag{5}$$

2.1.2 Electric Charge Formulation

An electric charge formulation can be obtained by using the Helmholz free energy, written in terms of mechanical strains $\boldsymbol{\varepsilon}$ and electric displacements $\mathbf{D}$, as potential energy instead of the electric Gibbs energy, such that the virtual variation of the potential energy is

$$\delta U(\boldsymbol{\varepsilon}, \mathbf{D}) = \int_{\Omega} \left(\delta\boldsymbol{\varepsilon}^{\mathrm{t}}\mathbf{c}^{D}\boldsymbol{\varepsilon} - \delta\boldsymbol{\varepsilon}^{\mathrm{t}}\mathbf{h}\mathbf{D} - \delta\mathbf{D}^{\mathrm{t}}\mathbf{h}^{\mathrm{t}}\boldsymbol{\varepsilon} + \delta\mathbf{D}^{\mathrm{t}}\boldsymbol{\beta}^{\varepsilon}\mathbf{D}\right)\mathrm{d}\Omega, \tag{6}$$

where $\mathbf{c}^{D}$, $\mathbf{h}$, and $\boldsymbol{\beta}^{\varepsilon}$ are the matrices of elastic (for constant electric displacement), piezoelectric, and dielectric (for constant mechanical strain) constants of the material.

In this case, the equations of motion are now written in terms of the generalized displacements $\mathbf{u}$ and electric displacements $\mathbf{D}_n$, such that

$$\begin{bmatrix} \mathbf{M}_{\mathrm{s}} + \mathbf{M}_{\mathrm{p}} & 0 \\ 0 & 0 \end{bmatrix} \begin{Bmatrix} \ddot{\mathbf{u}} \\ \ddot{\mathbf{D}}_n \end{Bmatrix} + \begin{bmatrix} \mathbf{K}_{\mathrm{us}} + \mathbf{K}_{\mathrm{up}}^{D} & -\mathbf{K}_{\mathrm{ud}} \\ -\mathbf{K}_{\mathrm{ud}}^{\mathrm{t}} & \mathbf{K}_{\mathrm{d}} \end{bmatrix} \begin{Bmatrix} \mathbf{u} \\ \mathbf{D}_n \end{Bmatrix} = \begin{Bmatrix} \mathbf{F}_{\mathrm{m}} \\ 0 \end{Bmatrix}, \tag{7}$$

where, as in the previous case, $\mathbf{M}_{\mathrm{s}}$ and $\mathbf{K}_{\mathrm{us}}$ are the mass and elastic stiffness matrices of the structure (without piezoelectric elements) and $\mathbf{M}_{\mathrm{p}}$ and $\mathbf{K}_{\mathrm{up}}^{D}$ are the mass and elastic (for constant electric displacements) stiffness matrices of the piezoelectric elements. $\mathbf{K}_{\mathrm{ud}}$ and $\mathbf{K}_{\mathrm{d}}$ are the piezoelectric and dielectric stiffnesses of the piezoelectric elements.

To account for the equipotential condition on the electrodes of each piezoelectric element, let us define the vectors of electric charges $\mathbf{q}_{\mathrm{p}}$ on the electrodes of piezoelectric elements (with uniform and equal material properties and thickness), such that

$$\mathbf{D}_n = \mathbf{B}_{\mathrm{p}}\mathbf{q}_{\mathrm{p}}, \quad \mathbf{B}_{\mathrm{p}} = \mathbf{L}_{\mathrm{p}}\mathbf{A}_{\mathrm{p}}^{-1}. \tag{8}$$

The boolean matrix $\mathbf{L}_{\mathrm{p}}$ has dimension $N \times N_{\mathrm{p}}$, where N is the number of spatial (nodal) points and N_{p} is the number of independent piezoelectric elements. $\mathbf{L}_{\mathrm{p}}$ allows to set an equal value to selected nodal electric displacements. $\mathbf{A}_{\mathrm{p}}$ is a diagonal matrix with the surface area of the electrodes of the piezoelectric elements.

Substituting Eq. (8) in Eq. (7) and pre-multiplying the second line of the resulting equation by $\mathbf{B}_{\mathrm{p}}^{\mathrm{t}}$ leads to

$$\begin{bmatrix} \mathbf{M}_{\mathrm{s}} + \mathbf{M}_{\mathrm{p}} & 0 \\ 0 & 0 \end{bmatrix} \begin{Bmatrix} \ddot{\mathbf{u}} \\ \ddot{\mathbf{q}}_{\mathrm{p}} \end{Bmatrix} + \begin{bmatrix} \mathbf{K}_{\mathrm{us}} + \mathbf{K}_{\mathrm{up}}^{D} & -\mathbf{K}_{\mathrm{uq}} \\ -\mathbf{K}_{\mathrm{uq}}^{\mathrm{t}} & \mathbf{K}_{\mathrm{q}} \end{bmatrix} \begin{Bmatrix} \mathbf{u} \\ \mathbf{q}_{\mathrm{p}} \end{Bmatrix} = \begin{Bmatrix} \mathbf{F}_{\mathrm{m}} \\ 0 \end{Bmatrix}, \tag{9}$$

where

$$\mathbf{K}_{\mathrm{uq}} = \mathbf{K}_{\mathrm{ud}} \mathbf{B}_{\mathrm{p}}, \quad \mathbf{K}_{\mathrm{q}} = \mathbf{B}_{\mathrm{p}}^{\mathrm{t}} \mathbf{K}_{\mathrm{d}} \mathbf{B}_{\mathrm{p}}. \tag{10}$$

2.2 Connection to Electric Circuits

It is worthwhile to analyze the connection of piezoelectric elements to electric circuits, specially when shunt circuits are considered for passive vibration control. To this end, it seems that an electric charge formulation is more appropriate since it is possible to relate the electric charges flowing between the piezoelectric elements electrodes with the electric charges flowing through the electric circuit. First, let us consider a set of simple but quite general electric circuits composed of an inductor, a resistor, and a voltage source. The equations of motion for such circuits can be found using d'Alembert's principle, such that the virtual work done by the inductors δT_{Lj}, resistors, δW_{Rj}, and voltage sources, δW_{Vj}, of the j-th electric circuit are

$$\delta T_{Lj} = -\delta q_{cj} L_{cj} \ddot{q}_{cj}, \quad \delta W_{Rj} = -\delta q_{cj} R_{cj} \dot{q}_{cj}, \quad \delta W_{Vj} = \delta q_{cj} V_{cj}, \tag{11}$$

where L_{cj}, R_{cj}, and V_{cj} are the inductance, resistance, and applied voltage of the j-th electric circuit. q_{cj} is the electric charge flowing through the j-th electric circuit. Combining the virtual work done by all circuits leads to

$$\begin{aligned} &\delta T_L = \sum_j \delta T_{Lj} = -\delta \mathbf{q}_c^{\mathrm{t}} \mathbf{L}_c \ddot{\mathbf{q}}_c, \quad \delta W_R = \sum_j \delta W_{Rj} = -\delta \mathbf{q}_c^{\mathrm{t}} \mathbf{R}_c \dot{\mathbf{q}}_c, \\ &\delta W_V = \sum_j \delta W_{Vj} = \delta \mathbf{q}_c^{\mathrm{t}} \mathbf{V}_c, \end{aligned} \tag{12}$$

where $\mathbf{q}_c$ is the vector of electric charges, $\mathbf{L}_c$ and $\mathbf{R}_c$ are diagonal matrices with the inductances and resistances of each circuit, and $\mathbf{V}_c$ is the vector of applied voltages.

Adding these virtual works to the electromechanical virtual works of previous section, such that

$$\delta T - \delta U + \delta W + \delta T_L + \delta W_R + \delta W_V = 0, \tag{13}$$

or, in terms of the generalized displacements,

$$\begin{aligned}\delta\mathbf{u}^{\mathrm{t}}\Big[(\mathbf{M}_{\mathrm{s}}+\mathbf{M}_{\mathrm{p}})\ddot{\mathbf{u}}+\Big(\mathbf{K}_{\mathrm{us}}+\mathbf{K}_{\mathrm{up}}^{D}\Big)\mathbf{u}-\mathbf{K}_{\mathrm{uq}}\mathbf{q}_{\mathrm{p}}-\mathbf{F}_{\mathrm{m}}\Big]\\ +\delta\mathbf{q}_{\mathrm{p}}^{\mathrm{t}}\Big(-\mathbf{K}_{\mathrm{uq}}^{\mathrm{t}}\mathbf{u}+\mathbf{K}_{\mathrm{q}}\mathbf{q}_{\mathrm{p}}\Big)+\delta\mathbf{q}_{c}^{\mathrm{t}}(\mathbf{L}_{c}\ddot{\mathbf{q}}_{c}+\mathbf{R}_{c}\dot{\mathbf{q}}_{c}-\mathbf{V}_{c})=0.\end{aligned} \tag{14}$$

Then, the connection between each piezoelectric element and a corresponding electric circuit is done by stating that the electric charges flowing from the piezoelectric element enter the circuit and vice-versa, such that

$$\mathbf{q}_{c}=\mathbf{q}_{\mathrm{p}}. \tag{15}$$

Thus, replacing $\mathbf{q}_c$ by $\mathbf{q}_{\mathrm{p}}$ in Eq. (14) leads to the following coupled equations of motion

$$\begin{aligned}&\begin{bmatrix}\mathbf{M}_{\mathrm{s}}+\mathbf{M}_{\mathrm{p}} & 0\\ 0 & \mathbf{L}_{c}\end{bmatrix}\begin{Bmatrix}\ddot{\mathbf{u}}\\ \ddot{\mathbf{q}}_{\mathrm{p}}\end{Bmatrix}+\begin{bmatrix}0 & 0\\ 0 & \mathbf{R}_{c}\end{bmatrix}\begin{Bmatrix}\dot{\mathbf{u}}\\ \dot{\mathbf{q}}_{\mathrm{p}}\end{Bmatrix}\\ &+\begin{bmatrix}\mathbf{K}_{\mathrm{us}}+\mathbf{K}_{\mathrm{up}}^{D} & -\mathbf{K}_{\mathrm{uq}}\\ -\mathbf{K}_{\mathrm{uq}}^{\mathrm{t}} & \mathbf{K}_{\mathrm{q}}\end{bmatrix}\begin{Bmatrix}\mathbf{u}\\ \mathbf{q}_{\mathrm{p}}\end{Bmatrix}=\begin{Bmatrix}\mathbf{F}_{\mathrm{m}}\\ \mathbf{V}_{c}\end{Bmatrix}.\end{aligned} \tag{16}$$

In this case, the solution for $\mathbf{u}$ and $\mathbf{q}_{\mathrm{p}}$ must be simultaneous, that is accounting for the electromechanical and circuit equations of motion. Notice that the passive components of the electric circuit $\mathbf{L}_c$ and $\mathbf{R}_c$ affect the equivalent piezoelectric force applied to the structure when an actuator with applied voltage is considered. For a simple actuator with applied voltage, that is with only a voltage source in the circuit ($\mathbf{L}_c=\mathbf{R}_c=0$), the second equation in Eq. (16) can be solved for $\mathbf{q}_{\mathrm{p}}$ leading to

$$\mathbf{q}_{\mathrm{p}}=\mathbf{K}_{\mathrm{q}}^{-1}\mathbf{V}_{c}+\mathbf{K}_{\mathrm{q}}^{-1}\mathbf{K}_{\mathrm{uq}}^{\mathrm{t}}\mathbf{u}, \tag{17}$$

which can be substituted in Eq. (16) such that it reduces to

$$(\mathbf{M}_{\mathrm{s}}+\mathbf{M}_{\mathrm{p}})\ddot{\mathbf{u}}+\Big[\mathbf{K}_{\mathrm{us}}+\Big(\mathbf{K}_{\mathrm{up}}^{D}-\mathbf{K}_{\mathrm{uq}}\mathbf{K}_{\mathrm{q}}^{-1}\mathbf{K}_{\mathrm{uq}}^{\mathrm{t}}\Big)\Big]\mathbf{u}=\mathbf{F}_{\mathrm{m}}+\mathbf{F}_{\mathrm{p}}, \tag{18}$$

where the equivalent piezoelectric force $\mathbf{F}_{\mathrm{p}}$ applied to the structure by the piezoelectric actuators is

$$\mathbf{F}_{\mathrm{p}}=\mathbf{K}_{\mathrm{uq}}\mathbf{K}_{\mathrm{q}}^{-1}\mathbf{V}_{c}. \tag{19}$$

From Eq. (18), the generalized displacements $\mathbf{u}$ induced by mechanical and piezoelectric equivalent forces can be evaluated. Then, the electric charges $\mathbf{q}_{\mathrm{p}}$ flowing between electrodes of the piezoelectric elements can be found using Eq. (17).

2.3 Design of Passive Resistive Shunt Circuits

In this section, the equations of motion (16) are reduced to the case of purely resistive shunt circuit by considering $\mathbf{L}_c = 0$ and $\mathbf{V}_c = 0$. It is then desired to use these equations to properly tune the values of electric resistance of the shunt circuits in order to maximize the added damping provided to a given vibration mode of interest.

For the sake of simplicity, only one piezoelectric patch connected to one resistive shunt circuit is considered. The structural response is represented only by the contribution of the vibration mode of interest, such that

$$\mathbf{u}(t) = \boldsymbol{\phi}_n \alpha_n(t), \tag{20}$$

where $\boldsymbol{\phi}_n$ is the n-th structural vibration mode, mass normalized, and α_n is the corresponding modal displacement. Then, the equations of motion (16) can be rewritten as

$$\ddot{\alpha}_n + \omega_n^2 \alpha_n - k_\mathrm{p} q = F_n, \tag{21}$$

$$R_c \dot{q} + k_e q - k_\mathrm{p} \alpha_n = 0, \tag{22}$$

where $k_\mathrm{p} = \boldsymbol{\phi}_n^\mathrm{t} \mathbf{K}_\mathrm{uq}$, $k_e = K_q$, and $\mathbf{F}_n = \boldsymbol{\phi}_n^\mathrm{t} \mathbf{F}_\mathrm{m}$. It is interesting to notice that ω_n is the n-th natural frequency for the structure considering an open circuit electric boundary condition for the piezoelectric patch ($R_c \to \infty$).

The computation of R_c is performed considering that the resistive shunt circuit behaves as a simple energy dissipation element and, thus, may modify (increase) the structural damping factor. Therefore, let us consider the free vibration case ($\mathbf{F}_\mathrm{m} = 0$) and quantify the effect of the shunt circuit on the dynamic behavior of the structure. Supposing a harmonic response $\alpha_n = \tilde{\alpha}_n \mathrm{e}^{j\omega t}$ and $q = \tilde{q}\,\mathrm{e}^{j\omega t}$,

$$\left(-\omega^2 + \omega_n^2\right)\tilde{\alpha}_n - k_\mathrm{p}\tilde{q} = 0, \tag{23}$$

$$(j\omega R_c + k_e)\tilde{q} - k_\mathrm{p}\tilde{\alpha}_n = 0. \tag{24}$$

Solving Eq. (24) for $\tilde{q}$ and substituting in Eq. (23) yields

$$\left[-\omega^2 + \left(\omega_n^2 - \frac{k_\mathrm{p}^2}{jR_c\omega + k_e}\right)\right]\tilde{\alpha}_n = 0. \tag{25}$$

Hence, the resistive shunt circuit leads to a complex natural frequency ω_n^* defined by

$$\omega_n^{*2} = \omega_n^2 - \frac{k_\mathrm{p}^2}{jR_c\omega + k_e}. \tag{26}$$

From this equation, it is possible to obtain relevant information about the electromechanical coupling and its effects. For instance, it is clear that the larger the electromechanical coupling coefficient (EMCC) between patch and structure for the vibration mode of interest, represented by k_{p}, the larger is the effect of the circuit on the structure. Besides, the cases of open circuit (oc) and short-circuit (sc) may be derived such that

$$\begin{aligned} \omega_n^{\mathrm{oc}\,2} &= \lim_{R_c \to \infty} \omega_n^{*2} = \omega_n^2, \\ \omega_n^{\mathrm{sc}\,2} &= \lim_{R_c \to 0} \omega_n^{*2} = \omega_n^2 - \frac{k_{\mathrm{p}}^2}{k_e}, \end{aligned} \tag{27}$$

where the effect of stiffness increase due to the induced potential is clear. One may also derive the following expression for the effective EMCC using

$$K_n^2 = \frac{\omega_n^{\mathrm{oc}\,2} - \omega_n^{\mathrm{sc}\,2}}{\omega_n^{\mathrm{oc}\,2}} = \frac{k_{\mathrm{p}}^2}{\omega_n^2 k_e}. \tag{28}$$

Introducing the nondimensional frequency ρ, it is possible to obtain

$$\rho = \frac{R_c \omega}{k_e} = R_c \omega C_{\mathrm{p}}^{\varepsilon}. \tag{29}$$

where $C_{\mathrm{p}}^{\varepsilon}$ is the piezoelectric patch electric capacitance for constant strain. Then, the complex natural frequency ω_n^* may be rewritten as function of the EMCC K_n^2 and nondimensional natural frequency ρ as

$$\omega_n^{*2} = \omega_n^2 \left(1 - \frac{K_n^2}{1 + j\rho} \right), \tag{30}$$

which, after some algebraic manipulations, may be written as

$$\omega_n^{*2} = \omega_{nr}^2 (1 + j\eta_n), \tag{31}$$

where ω_{nr} and η_n are defined as the real part of the natural frequency and the loss factor, respectively, which are

$$\omega_{nr}^2 = \omega_n^2 \left(1 - \frac{K_n^2}{1 + \rho^2} \right), \tag{32}$$

$$\eta_n = \frac{\rho K_n^2}{\left(1 - K_n^2\right) + \rho^2}. \tag{33}$$

Notice that the loss factor and the real part of the complex natural frequency are functions of the nondimensional frequency ρ. Therefore, it is desired to search for the value ρ_{op} that maximizes η_n. Making $\mathrm{d}\eta_n/\mathrm{d}\rho = 0$, the following solution is obtained

$$\rho_{\text{op}} = \sqrt{1 - K_n^2}, \tag{34}$$

such that the maximum loss factor is given by

$$\eta_n^{\max} = \frac{K_n^2}{2\sqrt{1 - K_n^2}}. \tag{35}$$

Combining Eqs. (29) and (34), an expression for the value of the electric resistance R_{op} that maximizes the loss factor at the natural frequency ω_n reads

$$R_{\text{op}} = \frac{k_e\sqrt{1 - K_n^2}}{\omega_n}. \tag{36}$$

Figure 1 shows theoretically attainable levels of material loss factor for standard piezoceramic materials in operation modes k_{33}, k_{15}, and k_{31}.

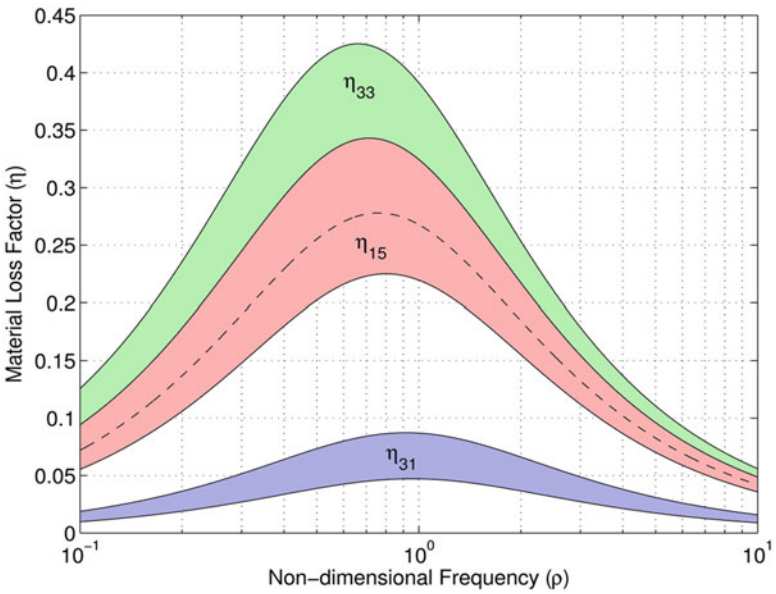

Fig. 1 Loss factor for standard piezoceramic materials using operation modes k_{33}, k_{15}, and k_{31} combined to resistive shunt circuits

2.4 Design of Passive Resonant Shunt Circuits

In the case of piezoelectric patches connected to resonant, or resistive-inductive (RL), shunt circuits, the circuit is no longer a simple energy dissipation element since the combination of circuit inductance and piezoelectric patch capacitance leads to an electrical resonance. On the other hand, this fact may be used in such a way that the circuit may absorb part of the energy generated by the piezoelectric material and, thus, behave as a dynamic vibration absorber. Therefore, the theory of dynamic vibration absorbers (Den Hartog 1985) is used.

To this end, the equations of motion (16) could be reduced to two degrees-of-freedom, one mechanical and one electrical. Thus, as in the previous section, the structural response is approximated by only the contribution of the vibration mode of interest. In the present case, the decomposition Eq. (20) is applied to Eq. (16) but maintaining both passive circuit elements ($R_c \neq 0$ and $L_c \neq 0$) while the voltage source is removed ($V = 0$). The equations of motion (16) are then reduced to

$$\ddot{\alpha}_n + \omega_n^2 \alpha_n - k_\mathrm{p} q = b_n p, \tag{37}$$

$$L_c \ddot{q} + R_c \dot{q} + k_e q - k_\mathrm{p} \alpha_n = 0. \tag{38}$$

The design of L_c and R_c aims to minimize the structure's frequency response amplitude. For that, let us suppose a mechanical excitation $p = \tilde{p}\, \mathrm{e}^{j\omega t}$, such that $\alpha_n = \tilde{\alpha}_n \mathrm{e}^{j\omega t}$ and $q = \tilde{q}\, \mathrm{e}^{j\omega t}$. It is also considered that the structural response will be measured by a displacement sensor that provides the output $y = \mathbf{c}_y \mathbf{u}$, where $\mathbf{c}_y$ is a vector that describes the output in terms of the contributions of the mechanical dof $\mathbf{u}$. Due to the harmonic excitation, the output is also in the form $y = \tilde{y}\, \mathrm{e}^{j\omega t}$, with $\tilde{y} = c_n \tilde{\alpha}_n$ and $c_n = \mathbf{c}_y \boldsymbol{\phi}_n$. The equations of motion (37) and (38) may be written as

$$\left(\omega_n^2 - \omega^2\right) \tilde{\alpha}_n - k_\mathrm{p} \tilde{q}_c = b_n \tilde{f}, \tag{39}$$

$$\left(-\omega^2 L_c + j\omega R_c + k_e\right) \tilde{q} - k_\mathrm{p} \tilde{\alpha}_n = 0. \tag{40}$$

Solving Eq. (40) for $\tilde{q}$, it is possible to write $\tilde{\alpha}_n$ and, thus $\tilde{y}$, as functions of the excitation amplitude $\tilde{f}$, where $\tilde{y} = H(\omega)\tilde{f}$,

$$H(\omega) = c_n b_n \frac{-\omega^2 L_c + k_e + j\omega R_c}{\omega^4 L_c - \omega^2\left(k_e + \omega_n^2 L_c\right) + \omega_n^2 k_e - k_\mathrm{p}^2 + j\omega R_c\left(\omega_n^2 - \omega^2\right)}. \tag{41}$$

The frequency response amplitude is defined as

$$|H(\omega)| = c_n b_n \left\{ \frac{\left(-\omega^2 L_c + k_e\right)^2 + \left(\omega R_c\right)^2}{\left[\omega^4 L_c - \omega^2\left(k_e + \omega_n^2 L\right) + \omega_n^2 k_e - k_\mathrm{p}^2\right]^2 + \omega R_c\left(\omega_n^2 - \omega^2\right)\Big]^2} \right\}^{1/2}, \tag{42}$$

and, for limited values of R_c, there is an anti-resonance at a frequency that is equal to the one of the electric circuit resonances, defined as $\omega_c = (k_e/L_c)^{1/2}$. One of the possible strategies to minimize the structural response amplitude at one of its resonance frequencies consists of designing the resonance frequency of the sub-system so that it coincides with the structure's resonance frequency of interest.

In this case, although both k_e and L_c may be designed, k_e is considered as a fixed parameter since it depends on physical and geometric properties of the piezoelectric patch. Therefore, it is desired to design a circuit that minimizes the structural response. This can be achieved by considering $\omega_c = \omega_n$, that allows us to compute the circuit inductance directly by

$$L_c = \frac{k_e}{\omega_n^2}. \tag{43}$$

The anti-resonance placed at ω_n is accompanied by two resonances, before and after ω_n, that must have their amplitudes controlled in order to minimize the amplification of the structural response in the case of frequency detuning. This can be achieved using the shunt circuit resistance to provide an equivalent damping to the two resonances. One possible methodology is to search for the resistance value that makes the amplitude at anti-resonance to be approximately equal to the one at two invariant frequencies, for which the amplitude is limited and independent on the resistance (Den Hartog 1985). These invariant frequencies can be evaluated through the following expression

$$\lim_{R_c \to 0} |H(\omega)|^2 = \lim_{R_c \to \infty} |H(\omega)|^2, \tag{44}$$

which, by substituting Eq. (42), leads to

$$\omega_{1,2}^2 = \frac{1}{2}\left[\omega_c^2 + \omega_n^2 \pm \sqrt{\left(\omega_c^2 - \omega_n^2\right)^2 + 2\omega_c^2\left(k_\mathrm{p}^2/k_e\right)}\right]. \tag{45}$$

The response amplitude at these invariant frequencies ω_1 and ω_2 and at the anti-resonance frequency ω_n are

$$|H(\omega_1)|^2 = \frac{R_c^2\omega_n^2}{k_\mathrm{p}^4} \quad \text{and} \quad |H(\omega_n)|^2 = \frac{2k_e}{k_\mathrm{p}^2\omega_n^2}. \tag{46}$$

By equalizing the two amplitudes, it is possible to find an expression for the shunt circuit resistance, such that

$$R_c = \frac{k_\mathrm{p}\sqrt{2k_e}}{\omega_n^2}. \tag{47}$$

Notice that it is written in terms of the equivalent coupling stiffness k_p, equivalent dielectric stiffness k_e, and structure's resonance frequency of interest ω_n.

2.5 *Piezoelectric Shunted Damping Example*

In this section, a case study of passive vibration control using piezoelectric patches connected to resistive and resonant shunt circuits is presented. The host structure is an Aluminum cantilever beam as shown in Fig. 2. The beam is lightly damped and this is accounted for using a constant modal damping factor of 0.5 %. The material properties of the Aluminum are: Young's modulus 70 GPa, Poisson ratio 0.35, and mass density 2700 kg m^{-3}. It is then desired to increase the structural damping of the host structure by using a passive control solution. Two piezoceramic patches (PZT5A) perfectly bonded to the host structure are connected to a shunt circuit, consisting of a resistance and an inductance. The width of both host structure and piezoceramic patches, not shown in the figure, is 25 mm. The material properties of the PZT5A piezoceramic are: $\overline{c}_{11}^D = c_{22}^D = 96.39\,\text{GPa}$, $\overline{c}_{12}^D = 51.22\,\text{GPa}$, $\overline{c}_{44}^D = \overline{c}_{55}^D = 39.63\,\text{GPa}$, $\overline{c}_{66}^D = 22.57\,\text{GPa}$, $\overline{h}_{31} = \overline{h}_{32} = -1.677 \times 10^9\,\text{N C}^{-1}$, $\overline{\beta}_{33}^{\varepsilon} = 104.5 \times 10^6\,\text{m F}^{-1}$, and $\rho^{\text{pzt}} = 7750\,\text{kg m}^{-3}$. The piezoceramic patches are fully covered by electrodes on the upper and lower surfaces. Electrodes at the interface with the host structure are considered to be grounded.

Figures 3 and 4 show the frequency response of the structure (between tip velocity and tip force) for three cases depending on the connection of the piezoelectric patches: (i) open-circuit, (ii) resistive shunt, (iii) resonant (resistive-inductive) shunt. The optimal value for the resistance in the resistive circuit was obtained using Eq. (36) leading to $R_c = 103\,\text{k}\Omega$. In the case of the resonant circuit, the optimal values for resistance and inductance were obtained using Eqs. (47) and (43), respectively, leading to $R_c = 18\,\text{k}\Omega$ and $L_c = 514\,\text{H}$. Notice that the resistance values were rounded in kΩ and the inductance value was manually fine tuned from 514 to 503 H.

It is possible to observe in Fig. 3 that both resistive and resonant shunt circuits allow to reduce the vibration amplitude only around a single resonance frequency with no modification of other resonances. In terms of vibration amplitude reduction performance, it is clear from Fig. 4 that the resonant shunt circuit, which may reduce the vibration amplitude in about 20 dB, is much more effective than the resistive one, which reduces amplitude in about 5 dB.

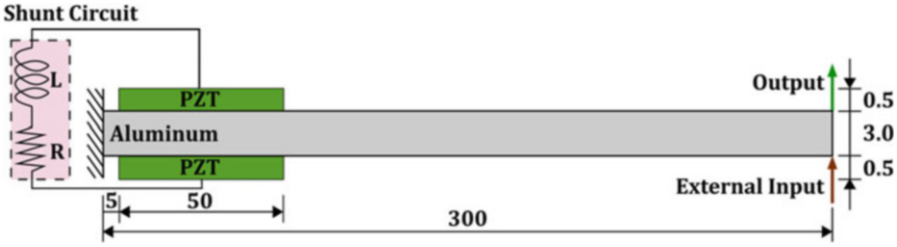

Fig. 2 Schematic representation of a cantilever beam with two piezoelectric patches connected to a resonant shunt circuit (dimensions in mm)

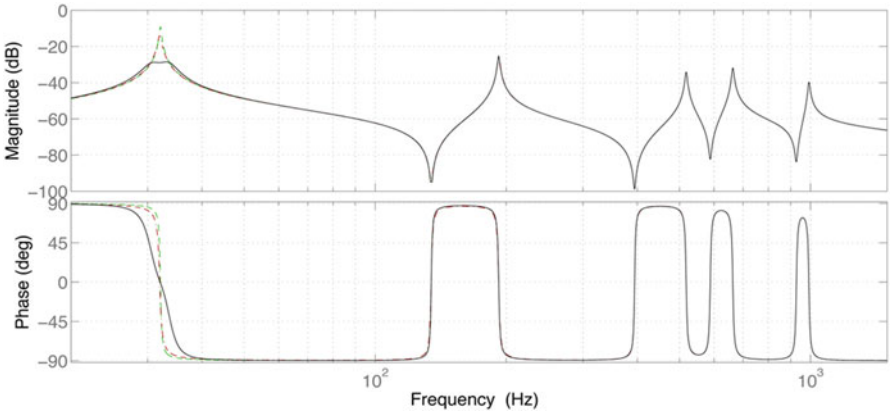

Fig. 3 Frequency response (*dashed*: open-circuit, *dash-dotted*: R shunt, *solid*: RL shunt) of the cantilever beam with piezoceramic patches connected to shunt circuit

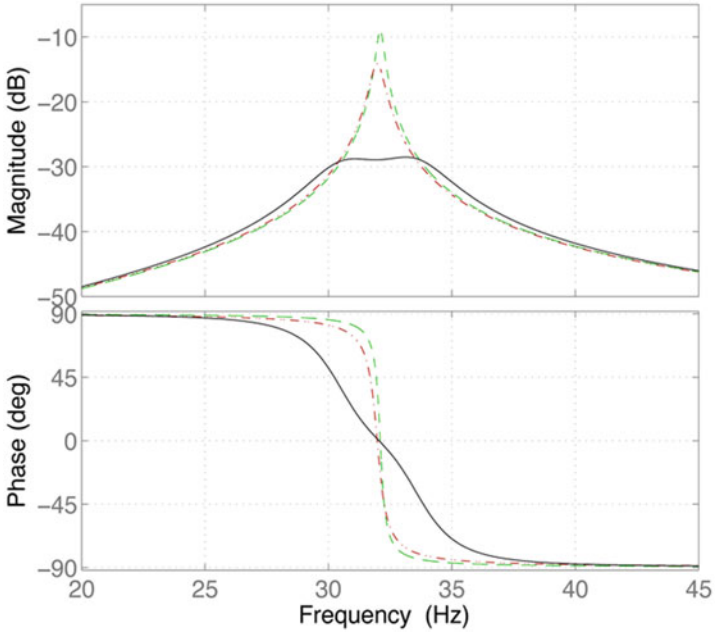

Fig. 4 Frequency response (*dashed*: open-circuit, *dash-dotted*: R shunt, *solid*: RL shunt) of the cantilever beam with piezoceramic patches connected to shunt circuit zoomed at the first resonance

3 Active Vibration Control Using Piezoelectric Materials

Since the mid-1980s, several studies focused on the use of distributed piezoelectric patches for the active vibration and noise control of thin plate-like structures (Bailey and Hubbard 1985). The main goal was to obtain a so-called adaptive structure with very integrated sensors and actuators so that adaptive/reconfigurable vibration mitigation solutions could be part of the structural design phase. Since then, several advances were observed in terms of predictive models, control design and optimization, experimental implementation and required power reduction with main focus on aeronautic and aerospace applications (Ahmadian and DeGuilio 2001; Reza Moheimani and Fleming 2006; Leo 2007). Some researchers also proposed combined active-passive vibration control strategies using piezoelectric patches (Tang et al. 2000; Santos and Trindade 2011).

In this section, a case study of active vibration control using piezoelectric patches as sensors and actuators is presented. The host structure is an Aluminum cantilever beam as shown in Fig. 5. The beam is lightly damped and this is accounted for using a constant modal damping factor of 0.5 %. The material properties of the Aluminum are: Young's modulus 70 GPa, Poisson ratio 0.35, and mass density 2700 kg m^{-3}. It is then desired to increase the structural damping of the host structure by using an active control solution. Two piezoceramic patches (PZT5A) perfectly bonded to the host structure are considered as sensor and actuator and these are connected by an active controller, consisting of a control unit and a power amplifier. The width of both host structure and piezoceramic patches, not shown in the figure, is 25 mm. The material properties of the PZT5A piezoceramic are: $\overline{c}_{11}^{D} = c_{22}^{D} = 96.39\,\text{GPa}, \overline{c}_{12}^{D} = 51.22\,\text{GPa}, \overline{c}_{44}^{D} = \overline{c}_{55}^{D} = 39.63\,\text{GPa}$, $\overline{c}_{66}^{D} = 22.57\,\text{GPa}, \overline{h}_{31} = \overline{h}_{32} = -1.677 \times 10^{9}\,\text{NC}^{-1}, \overline{\beta}_{33}^{\varepsilon} = 104.5 \times 10^{6}\,\text{mF}^{-1}$, and $\rho^{\text{pzt}} = 7750\,\text{kg}\,\text{m}^{-3}$. The piezoceramic patches are fully covered by electrodes on the upper and lower surfaces. Electrodes at the interface with the host structure are considered to be grounded. The piezoceramic sensor is considered to be connected to the control unit through a high impedance input such that it provides a voltage (electric potential) signal. The control voltage is imposed to the upper electrode of the piezoceramic actuator.

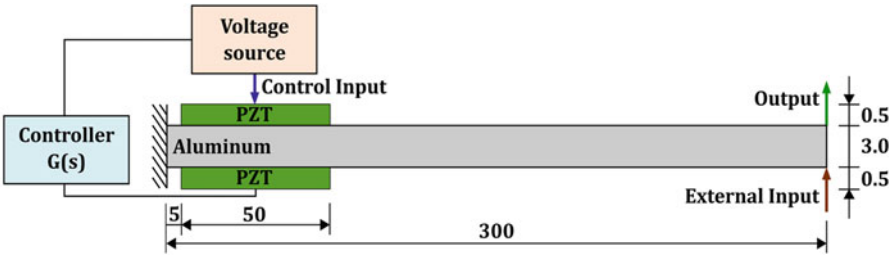

Fig. 5 Schematic representation of a cantilever beam with two piezoelectric patches serving as sensor and actuator connected to an active controller (dimensions in mm)

A coupled second-order model is constructed for the host structure with piezoelectric patches using the finite element method leading to

$$\begin{bmatrix} \mathbf{M}_t & \mathbf{0} & \mathbf{0} \\ \mathbf{0} & 0 & 0 \\ \mathbf{0} & 0 & 0 \end{bmatrix} \begin{Bmatrix} \ddot{\mathbf{u}} \\ \ddot{V}_\mathrm{s} \\ \ddot{V}_\mathrm{a} \end{Bmatrix} + \begin{bmatrix} \mathbf{K}_\mathrm{us} + \mathbf{K}^E_\mathrm{ups} + \mathbf{K}^E_\mathrm{upa} & -\overline{\mathbf{K}}_\mathrm{uvs} & -\overline{\mathbf{K}}_\mathrm{uva} \\ -\overline{\mathbf{K}}^\mathrm{t}_\mathrm{uvs} & -\overline{\mathbf{K}}_\mathrm{vs} & 0 \\ -\overline{\mathbf{K}}^\mathrm{t}_\mathrm{uva} & 0 & -\overline{\mathbf{K}}_\mathrm{va} \end{bmatrix} \begin{Bmatrix} \mathbf{u} \\ V_\mathrm{s} \\ V_\mathrm{a} \end{Bmatrix} = \begin{Bmatrix} \mathbf{F}_\mathrm{m} \\ 0 \\ 0 \end{Bmatrix}. \tag{48}$$

The control voltage applied to the actuator V_a is prescribed and thus the third line of Eq. (48) is automatically satisfied and the terms containing V_a in the first line can be moved to the right side. As for the sensor voltage V_s, it may be written in terms of the structure's displacements vector as

$$V_\mathrm{s} = -\overline{\mathbf{K}}^{-1}_\mathrm{vs}\,\overline{\mathbf{K}}^\mathrm{t}_\mathrm{uvs}\mathbf{u}, \tag{49}$$

and then substituted in the first equation such that

$$\mathbf{M}_t\ddot{\mathbf{u}} + \mathbf{D}\dot{\mathbf{u}} + \mathbf{K}_\mathrm{ut}\mathbf{u} = \mathbf{F}_\mathrm{m} + \overline{\mathbf{K}}_\mathrm{uva}V_\mathrm{a}, \tag{50}$$

where $\mathbf{K}_\mathrm{ut} = \mathbf{K}_\mathrm{us} + \mathbf{K}^E_\mathrm{ups} + \mathbf{K}^E_\mathrm{upa} + \overline{\mathbf{K}}_\mathrm{uvs}\overline{\mathbf{K}}^{-1}_\mathrm{vs}\overline{\mathbf{K}}^\mathrm{t}_\mathrm{uvs}$ and a damping matrix $\mathbf{D}$ is included a posteriori.

Applying the methodology presented previously, the mechanical force is considered as a perturbation input such that $\mathbf{F}_\mathrm{m} = \mathbf{b}_\mathrm{p}p$, the voltage induced in the piezoceramic sensor is considered as the measurement output such that $y = V_\mathrm{s} = \mathbf{c}_y\mathbf{u}$, with $\mathbf{c}_y = -\overline{K}^{-1}_\mathrm{vs}\overline{\mathbf{K}}^\mathrm{t}_\mathrm{uvs}$, and the voltage applied to the piezoceramic actuator V_a is considered as the control input, such that $\mathbf{b}_f = \overline{\mathbf{K}}_\mathrm{uva}$.

In order to simplify the control design, a model reduction is performed using projection onto a reduced undamped modal basis, truncated to the vibration modes of interest $\boldsymbol{\phi}_j$, solution of $\left(-\omega_j^2\mathbf{M}_t + \mathbf{K}_\mathrm{ut}\right)\boldsymbol{\phi}_j = 0$. As discussed previously, it is very important to well represent the anti-resonance frequencies (or system zeros) in the control design. The low-frequency response of the neglected higher-frequencies vibration modes may have an important contribution to the location of the system zeros. Therefore, it is advisable to keep some vibration modes outside the frequency range of interest. The modal basis can also be enriched using the static contribution of the neglected vibration modes $\boldsymbol{\phi}_\mathrm{s} = \mathbf{K}^{-1}_\mathrm{ut}\overline{\mathbf{K}}_\mathrm{uva}$. The structure's displacements are then approximated as $\mathbf{u} \approx \sum_j \boldsymbol{\phi}_j\alpha_j$ and, thus, the reduced equations of motion are written as

$$\begin{cases} \ddot{\boldsymbol{\alpha}} + \boldsymbol{\Lambda}\dot{\boldsymbol{\alpha}} + \boldsymbol{\Omega}^2\boldsymbol{\alpha} = \boldsymbol{\Phi}^\mathrm{t}\mathbf{F}_\mathrm{m} + \boldsymbol{\Phi}^\mathrm{t}\overline{\mathbf{K}}_\mathrm{uva}V_\mathrm{a}, \\ V_\mathrm{s} = -\overline{K}^{-1}_\mathrm{vs}\overline{\mathbf{K}}^\mathrm{t}_\mathrm{uvs}\boldsymbol{\Phi}\boldsymbol{\alpha}. \end{cases} \tag{51}$$

For the sake of simplicity, in the present case, only the first six vibration modes (bending modes for all but the third and fifth ones that correspond to torsion modes) are kept in the reduced-order model.

Then, in order to make use of standard control system tools, the second-order reduced system Eq. (51) is rewritten in the following state-space form

$$\begin{cases} \dot{\mathbf{z}} = \mathbf{A}\mathbf{z} + \mathbf{B}_{\mathrm{p}} p + \mathbf{B}_c V_{\mathrm{a}}, \\ V_{\mathrm{s}} = \mathbf{C}_y \mathbf{z}, \end{cases} \tag{52}$$

where

$$\mathbf{z} = \begin{bmatrix} \boldsymbol{\alpha} \\ \dot{\boldsymbol{\alpha}} \end{bmatrix}, \quad \mathbf{A} = \begin{bmatrix} \mathbf{0} & \mathbf{I} \\ -\boldsymbol{\Omega}^2 & -\boldsymbol{\Lambda} \end{bmatrix}, \quad \mathbf{B}_{\mathrm{p}} = \begin{bmatrix} \mathbf{0} \\ \boldsymbol{\Phi}^{\mathrm{t}} \mathbf{b}_{\mathrm{p}} \end{bmatrix}, \quad \mathbf{B}_c = \begin{bmatrix} \mathbf{0} \\ \boldsymbol{\Phi}^{\mathrm{t}} \overline{\mathbf{K}}_{\mathrm{uva}} \end{bmatrix}, \tag{53}$$
$$\mathbf{C}_y = \begin{bmatrix} -\overline{K}_{\mathrm{vs}}^{-1} \overline{\mathbf{K}}_{\mathrm{uvs}}^{\mathrm{t}} \boldsymbol{\Phi} & \mathbf{0} \end{bmatrix}.$$

Then, the transfer function between sensor and actuator used in the control system reads $H_c(s) = \mathbf{C}_y (s\mathbf{I} - \mathbf{A})^{-1} \mathbf{B}_c$. In what follows, two simple control laws are designed based on this information: (i) Direct Velocity Feedback (DVF) and (ii) Positive Position Feedback (PPF). The control design is performed here with the aid of *rltool* Graphical User Interface of Control System Toolbox of MATLAB(R). For the DVF control, a real zero at $s = 0$ is added leading to a simple differentiator. For the PPF control, two complex conjugate poles near the open-loop poles corresponding to the vibration mode to be controlled are added.

Figure 6a shows the root locus of the closed-loop system. From the root locus, one may conclude that very large damping values could be obtained, in particular for the second and fourth modes (which are the second and third bending modes). However, it is important to notice that large values of control gains may not be realistic since they would require large control voltages that may not be feasible due to the maximum electric field supported by the piezoelectric patches and also the voltage and power demanded to the power amplifier (Trindade, Benjeddou, and Ohayon 2001). In the present case, it is assumed that the control voltage should not exceed 250 V (which leads to an applied electric field of 500 V/mm in the 0.5 mm thick piezoelectric patches). Commercial power amplifiers allow the application of such voltages for a limited frequency range and patches capacitance. For some applications, the energy consumption could also be used to design and analysis of control strategies (Wang and Inman 2011). There are also alternatives to reduce the maximum voltage required for a given performance (Tang et al. 2000; Sirohi and Chopra 2001; Santos and Trindade 2011).

Considering the maximum voltage limitation, the maximum feasible control gain is approximately $g = 5000$ Vs/V. Then, the control performance is much weaker than the ones allowed by the control law alone. Nevertheless, a feasible DVF control still yields reasonable performance in terms of added structural

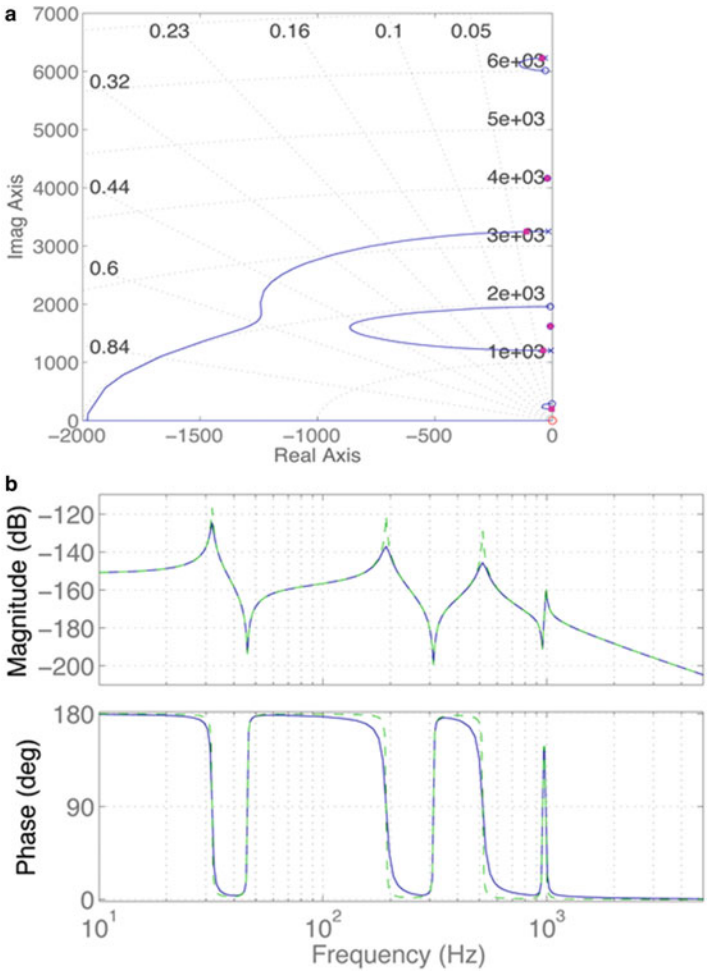

Fig. 6 (**a**) Root locus and (**b**) frequency response (*solid*: open loop, *dashed*: closed-loop) of the cantilever beam with piezoceramic patches and DVF control law

damping. Indeed, the modal damping factors of first three bending modes are increased from 0.5 to 1.2 %, 3.3 %, and 3.4 %, respectively. This also leads to a reduction in the vibration amplitude as shown in Fig. 6b.

Figure 7a, b shows, respectively, the impulsive time responses of the open-loop and closed-loop sensor voltages and the control voltage applied to the actuator.

As discussed previously a simple output feedback law, as DVF, is not able to focus on given vibration modes. The selection/prioritization of the modes that are better controlled depends mainly on the positioning of sensor and actuator and its relation with the mode shapes. This is one of the reasons why the Positive Position Feedback (PPF) may be very useful for structural vibration control. Provided that

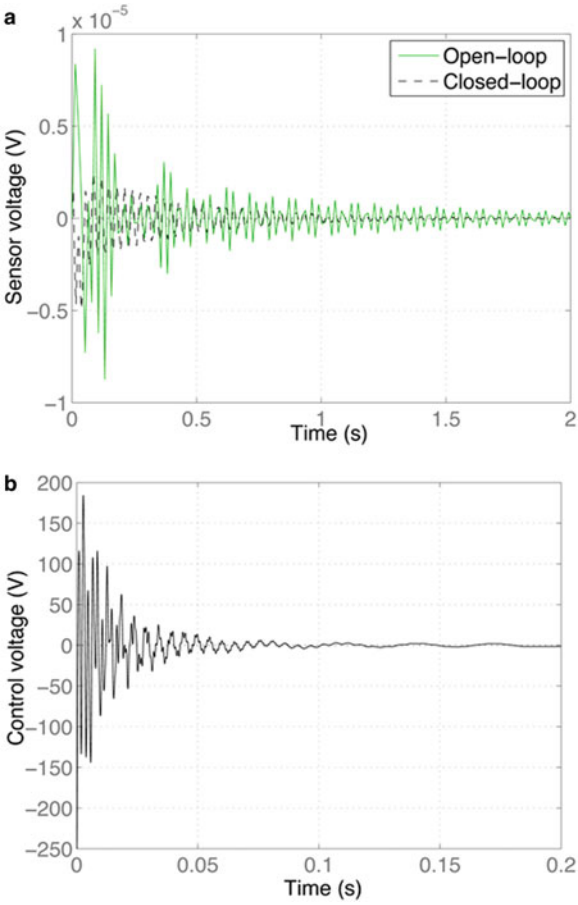

Fig. 7 Impulse responses of (**a**) sensor voltage (*solid*: open loop, *dashed*: closed-loop) and (**b**) control voltage of the cantilever beam with piezoceramic patches and DVF control law

the natural frequencies (in fact, the open-loop poles) are known and available for proper tuning of the control parameters ω_f and ξ_f, the PPF control should allow to focus on a given vibration mode and, thus, to minimize the modification of other modes and optimize the use of the control energy.

As an example, a PPF control law focusing on the first vibration mode is considered for the cantilever beam with piezoelectric patches. The first vibration mode natural frequency is approximately 32 Hz (201 rad/s). Based on this information and with the aid of simulations in *rltool*, the PPF parameters are set to $\omega_f = 205\,\text{rad/s}$ and $\xi_f = 0.2$. Figure 8a shows the root locus of the closed-loop system in which it is possible to notice that the PPF does allow to completely modify the path of the closed-loop poles such that the first vibration mode can now be substantially damped while the second and third bending modes are much less modified. For a PPF control gain of $g = 38\ \text{V/V}$, the vibration amplitude at the first natural frequency is greatly reduced as shown in Fig. 8b.

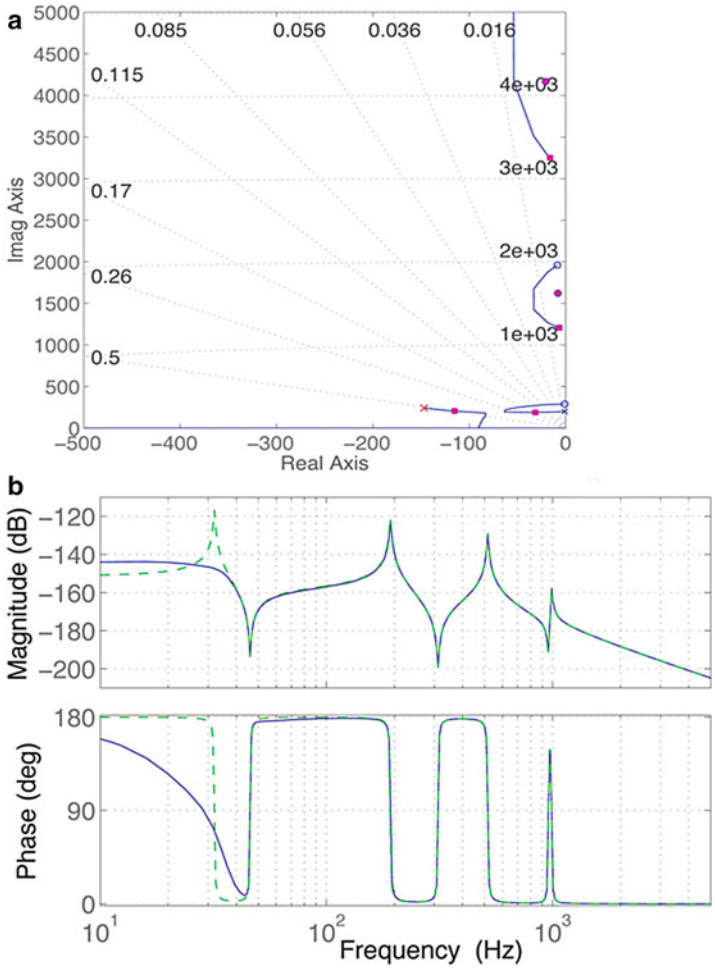

Fig. 8 (**a**) Root locus and (**b**) frequency response (*solid*: open loop, *dashed*: closed-loop) of the cantilever beam with piezoceramic patches and PPF control law

It is possible to observe in Fig. 9a, however, that the overshoot of the impulsive time response is increased in closed-loop although the settling time is reduced. Figure 9b also shows the control voltage required for such performance.

It is worthwhile to notice that, as discussed briefly in previous section, the obtained closed-loop control performance for both DVF and PPF control laws depend on the perturbation level of the system. Although theoretically these control performances are attainable, for higher excitation levels, the sensor output is also increased and so is the control voltage required to achieve such performances. In the present case, a perturbation force leading to a displacement amplitude of the order of the host structure thickness was used. To avoid saturation of the control voltage and its unpredictable effects, the control gain should be diminished as the perturbation level increases, leading to less performing vibration control.

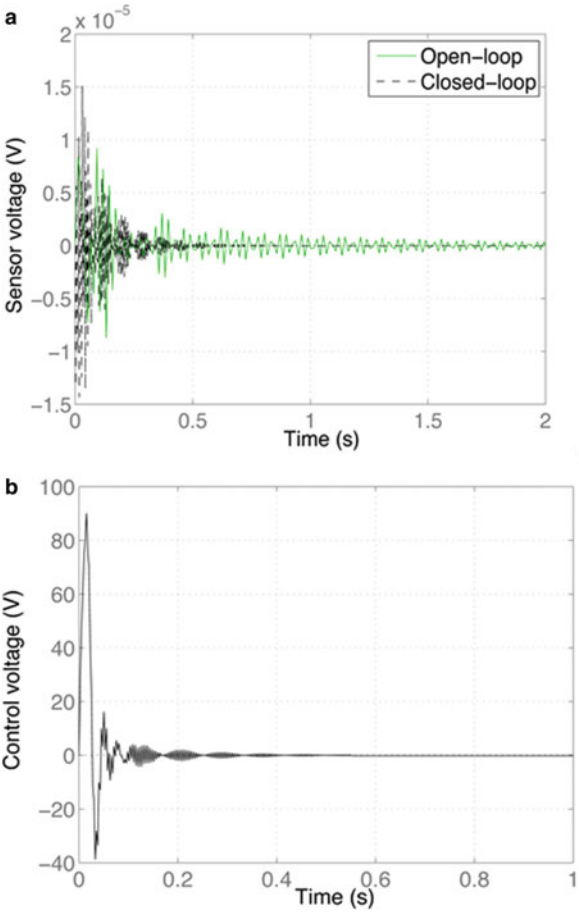

Fig. 9 Impulse responses of (**a**) sensor voltage (*solid*: open loop, *dashed*: closed-loop) and (**b**) control voltage of the cantilever beam with piezoceramic patches and PPF control law

References

M. Ahmadian, A.P. DeGuilio, Recent advances in the use of piezoceramics for vibration suppression. Shock Vib. Dig. **33**(1), 15–22 (2001)

T. Bailey, J.E. Hubbard Jr., Distributed piezoelectric-polymer active vibration control of a cantilever beam. AIAA J. **8**(5), 605–611 (1985)

W.W. Clark, Vibration control with state-switched piezoelectric materials. J. Intel. Mater. Syst. Struct. **11**(4), 263–271 (2000)

J.P. Den Hartog, *Mechanical Vibrations*, 4th edn. (Dover, New York, 1985)

T.C. Godoy, M.A. Trindade, Modeling and analysis of laminate composite plates with embedded active-passive piezoelectric networks. J. Sound Vib. **330**(2), 194–216 (2011)

N.W. Hagood, A. von Flotow, Damping of structural vibrations with piezoelectric materials and passive electrical networks. J. Sound Vib. **146**(2), 243–268 (1991)

M. Lallart, E. Lefeuvre, C. Richard, D. Guyomar, Self-powered circuit for broadband, multimodal piezoelectric vibration control. Sens. Actuators A **143**, 377–382 (2008)

D.J. Leo, *Engineering Analysis of Smart Material Systems* (Wiley, New York, 2007)

G.A. Lesieutre, Vibration damping and control using shunted piezoelectric materials. Shock Vib. Dig. **30**(3), 187–195 (1998)
L. Meirovitch, *Dynamics and Control of Structures* (Wiley, New York, 1990)
A. Preumont, *Vibration Control of Active Structures: An Introduction* (Kluwer Academic, Dordrecht, 1997)
A. Preumont, *Mechatronics: Dynamics of Electromechanical and Piezoelectric Systems* (Springer, Dordrecht, 2006)
S.O. Reza Moheimani, A survey of recent innovations in vibration damping and control using shunted piezoelectric transducers. IEEE Trans. Contr. Syst. Technol. **11**(4), 482–494 (2003)
S.O. Reza Moheimani, A.J. Fleming, *Piezoelectric Transducers for Vibration Control and Damping* (Springer, London, 2006)
H.F.L. Santos, M.A. Trindade, Structural vibration control using extension and shear active–passive piezoelectric networks including sensitivity to electrical uncertainties. J. Braz. Soc. Mech. Sci. Eng. **33**(3), 287–301 (2011)
J. Sirohi, I. Chopra, Actuator power reduction using L-C oscillator circuits. J. Intel. Mater. Syst. Struct. **12**(12), 867–877 (2001)
J. Tang, Y. Liu, K.W. Wang, Semiactive and active–passive hybrid structural damping treatments via piezoelectric materials. Shock Vib. Dig. **32**(3), 189–200 (2000)
M.A. Trindade, A. Benjeddou, Effective electromechanical coupling coefficients of piezoelectric adaptive structures: critical evaluation and optimization. Mech. Adv. Mater. Struct. **16**(3), 210–223 (2009)
M.A. Trindade, C.E.B. Maio, Multimodal passive vibration control of sandwich beams with shunted shear piezoelectric materials. Smart Mater. Struct. **17**(5), 055015 (2008)
M.A. Trindade, A. Benjeddou, R. Ohayon, Piezoelectric active vibration control of damped sandwich beams. J. Sound Vib. **246**(4), 653–677 (2001)
F.A.C. Viana, V. Steffen Jr., Multimodal vibration damping through piezoelectric patches and optimal resonant shunt circuits. J. Braz. Soc. Mech. Sci. **28**(3), 293–310 (2006)
Y. Wang, D.J. Inman, Comparison of control laws for vibration suppression based on energy consumption. J. Intel. Mater. Syst. Struct. **22**(8), 795–809 (2011)